

### FEATURES

- Qualified for automotive applications
- FET input amplifier
- 1 pA input bias current
- Low cost
- High speed: 145 MHz,  $-3$  dB bandwidth ( $G = +1$ )
- 180 V/ $\mu$ s slew rate ( $G = +2$ )
- Low noise
  - 7 nV/ $\sqrt{\text{Hz}}$  ( $f = 10$  kHz)
  - 0.6 fA/ $\sqrt{\text{Hz}}$  ( $f = 10$  kHz)
- Wide supply voltage range: 5 V to 24 V
- Single-supply and rail-to-rail output
- Low offset voltage 1.5 mV maximum
- High common-mode rejection ratio:  $-100$  dB
- Excellent distortion specifications
- SFDR  $-88$  dBc @ 1 MHz
- Low power: 6.4 mA/amplifier typical supply current
- No phase reversal
- Small packaging: SOIC-8, SOT-23-5, and MSOP-8

### GENERAL DESCRIPTION

The AD8065/AD8066<sup>1</sup> FastFET™ amplifiers are voltage feedback amplifiers with FET inputs offering high performance and ease of use. The AD8065 is a single amplifier, and the AD8066 is a dual amplifier. These amplifiers are developed in the Analog Devices, Inc. proprietary XFCB process and allow exceptionally low noise operation (7.0 nV/ $\sqrt{\text{Hz}}$  and 0.6 fA/ $\sqrt{\text{Hz}}$ ) as well as very high input impedance.

With a wide supply voltage range from 5 V to 24 V, the ability to operate on single supplies, and a bandwidth of 145 MHz, the AD8065/AD8066 are designed to work in a variety of applications. For added versatility, the amplifiers also contain rail-to-rail outputs.

Despite the low cost, the amplifiers provide excellent overall performance. The differential gain and phase errors of 0.02% and 0.02°, respectively, along with 0.1 dB flatness out to 7 MHz, make these amplifiers ideal for video applications. Additionally, they offer a high slew rate of 180 V/ $\mu$ s, excellent distortion (SFDR of  $-88$  dBc @ 1 MHz), extremely high common-mode rejection of  $-100$  dB, and a low input offset voltage of 1.5 mV maximum under warmed up conditions. The AD8065/AD8066 operate using only a 6.4 mA/amplifier typical supply current and are capable of delivering up to 30 mA of load current.

<sup>1</sup> Protected by U. S. Patent No. 6,262,633.

**Rev. L** **Document Feedback**  
 Information furnished by Analog Devices is believed to be accurate and reliable. However, no responsibility is assumed by Analog Devices for its use, nor for any infringements of patents or other rights of third parties that may result from its use. Specifications subject to change without notice. No license is granted by implication or otherwise under any patent or patent rights of Analog Devices. Trademarks and registered trademarks are the property of their respective owners.

### APPLICATIONS

- Automotive driver assistance systems
- Photodiode preamps
- Filters
- A/D drivers
- Level shifting
- Buffering

### CONNECTION DIAGRAMS



Figure 1.

The AD8065/AD8066 are high performance, high speed, FET input amplifiers available in small packages: SOIC-8, MSOP-8, and SOT-23-5. They are rated to work over the industrial temperature range of  $-40^{\circ}\text{C}$  to  $+85^{\circ}\text{C}$ .

The AD8065WARTZ-R7 is fully qualified for automotive applications. It is rated to operate over the extended temperature range ( $-40^{\circ}\text{C}$  to  $+105^{\circ}\text{C}$ ), up to a maximum supply voltage range of  $\pm 5$  V only.

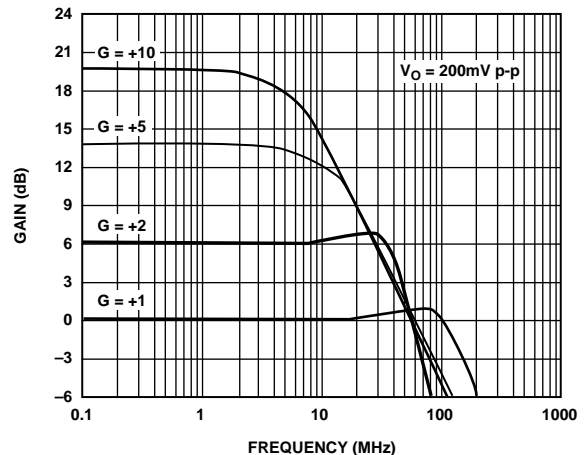


Figure 2. Small Signal Frequency Response

## TABLE OF CONTENTS

Features .....	1	Wideband Operation .....	21
Applications .....	1	Input Protection .....	21
Connection Diagrams .....	1	Thermal Considerations .....	22
General Description .....	1	Input and Output Overload Behavior .....	22
Revision History .....	3	Layout, Grounding, and Bypassing Considerations .....	23
Specifications $\pm 5$ V .....	4	Power Supply Bypassing .....	23
Specifications $\pm 12$ V .....	6	Grounding .....	23
Specifications +5 V .....	7	Leakage Currents .....	23
Absolute Maximum Ratings .....	9	Input Capacitance .....	23
Maximum Power Dissipation .....	9	Output Capacitance .....	23
Output Short Circuit .....	9	Input-to-Output Coupling .....	24
ESD Caution .....	9	Wideband Photodiode Preamp .....	24
Typical Performance Characteristics .....	10	High Speed JFET Input Instrumentation Amplifier .....	25
Test Circuits .....	17	Video Buffer .....	26
Theory of Operation .....	20	Outline Dimensions .....	27
Closed-Loop Frequency Response .....	20	Ordering Guide .....	28
Noninverting Closed-Loop Frequency Response .....	20	Automotive Products .....	28
Inverting Closed-Loop Frequency Response .....	20		

**REVISION HISTORY****1/2019—Rev. K to Rev. L**

Changed AD8065WARTZ-REEL7 to  
AD8065WARTZ-R7 ..... Throughout

**8/2016—Rev. J to Rev. K**

Updated Outline Dimensions.....27  
Changes to Ordering Guide.....28

**8/2010—Rev. I to Rev. J**

Changes to Features Section, Applications Section, and General  
Description Section..... 1  
Change to Table 1 .....4  
Change to Table 3 .....7  
Changes to Table 4 .....9  
Changes to Figure 9.....10  
Changes to Inverting Closed-Loop Frequency Response  
Section .....20  
Moved Leakage Currents Section, Input Capacitance Section,  
and Output Capacitance Section.....23  
Moved Input-to-Input Coupling Section, Wideband  
Photodiode Preamp Section, and Figure 59 .....24  
Changes to Table 5 .....25  
Moved Figure 60 and High Speed JFET Input Instrumentation  
Amplifier Section .....25  
Updated Outline Dimensions.....27  
Changes to Ordering Guide.....28  
Added Automotive Products Section .....28

**3/2009—Rev. H to Rev. I**

Changes to High Speed JFET Input Instrumentation Amplifier  
Section .....23  
Updated Outline Dimensions.....24

**9/2008—Rev. G to Rev. H**

Deleted Usable Range Parameter, Table 1 .....3  
Deleted Usable Range Parameter, Table 2 .....4  
Deleted Usable Range Parameter, Table 3 .....5  
Changes to Layout.....6  
Changes to Input and Output Overload Behavior Section.....19  
Changes to Table 5 Expressions Column .....22

**1/2006—Rev. F to Rev. G**

Changes to Ordering Guide.....26

**12/2005—Rev. E to Rev. F**

Updated Format..... Universal  
Changes to Features ..... 1

Changes to General Description ..... 1  
Changes to Figure 22 through Figure 27.....11  
Updated Outline Dimensions.....25  
Changes to Ordering Guide.....26

**2/2004—Rev. D to Rev. E.**

Updated Format ..... Universal  
Updated Figure 56..... 21  
Updated Outline Dimensions..... 25  
Updated Ordering Guide ..... 26

**11/2003—Rev. C to Rev. D.**

Changes to Features .....1  
Changes to Connection Diagrams.....1  
Updated Ordering Guide .....5  
Updated Outline Dimensions..... 22

**4/2003—Rev. B to Rev. C.**

Added SOIC-8 (R) for the AD8065 .....4

**2/2003—Rev. A to Rev. B.**

Changes to Absolute Maximum Ratings.....4  
Changes to Test Circuit 10 ..... 14  
Changes to Test Circuit 11 ..... 15  
Changes to Noninverting Closed-Loop Frequency Response 16  
Changes to Inverting Closed-Loop Frequency Response ..... 16  
Updated Figure 6 ..... 18  
Changes to Figure 7 ..... 19  
Changes to Figure 10 ..... 21  
Changes to Figure 11 ..... 22  
Changes to High Speed JFET Instrumentation Amplifier ..... 22  
Changes to Video Buffer ..... 22

**8/2002—Rev. 0 to Rev. A.**

Added AD8066..... Universal  
Added SOIC-8 (R) and MSOP-8 (RM) ..... 1  
Edits to General Description ..... 1  
Edits to Specifications.....2  
New Figure 2.....5  
Changes to Ordering Guide.....5  
Edits to TPCs 18, 25, and 28 .....8  
New TPC 36..... 11  
Added Test Circuits 10 and 11 ..... 14  
MSOP (RM-8) Added ..... 23

SPECIFICATIONS  $\pm 5$  V

@  $T_A = 25^\circ\text{C}$ ,  $V_S = \pm 5$  V,  $R_L = 1$  k $\Omega$ , unless otherwise noted.

Table 1.

Parameter	Conditions	Min	Typ	Max	Unit
<b>DYNAMIC PERFORMANCE</b>					
–3 dB Bandwidth	$G = +1$ , $V_O = 0.2$ V p-p (AD8065)	100	145		MHz
	AD8065WARTZ only: $T_{MIN} - T_{MAX}$	88			MHz
Bandwidth for 0.1 dB Flatness	$G = +1$ , $V_O = 0.2$ V p-p (AD8066)	100	120		MHz
	$G = +2$ , $V_O = 0.2$ V p-p		50		MHz
Input Overdrive Recovery Time	$G = +2$ , $V_O = 2$ V p-p		42		MHz
	$G = +2$ , $V_O = 0.2$ V p-p		7		MHz
Output Recovery Time	$G = +1$ , $-5.5$ V to $+5.5$ V		175		ns
Slew Rate	$G = -1$ , $-5.5$ V to $+5.5$ V		170		ns
	$G = +2$ , $V_O = 4$ V step	130	180		V/ $\mu$ s
Settling Time to 0.1%	AD8065WARTZ only: $T_{MIN} - T_{MAX}$	155			V/ $\mu$ s
	$G = +2$ , $V_O = 2$ V step		55		ns
	$G = +2$ , $V_O = 8$ V step		205		ns
<b>NOISE/HARMONIC PERFORMANCE</b>					
SFDR	$f_C = 1$ MHz, $G = +2$ , $V_O = 2$ V p-p		–88		dBc
	$f_C = 5$ MHz, $G = +2$ , $V_O = 2$ V p-p		–67		dBc
	$f_C = 1$ MHz, $G = +2$ , $V_O = 8$ V p-p		–73		dBc
Third-Order Intercept	$f_C = 10$ MHz, $R_L = 100$ $\Omega$		24		dBm
Input Voltage Noise	$f = 10$ kHz		7		nV/ $\sqrt{\text{Hz}}$
Input Current Noise	$f = 10$ kHz		0.6		fA/ $\sqrt{\text{Hz}}$
Differential Gain Error	NTSC, $G = +2$ , $R_L = 150$ $\Omega$		0.02		%
Differential Phase Error	NTSC, $G = +2$ , $R_L = 150$ $\Omega$		0.02		Degrees
<b>DC PERFORMANCE</b>					
Input Offset Voltage	$V_{CM} = 0$ V, SOIC package		0.4	1.5	mV
	AD8065WARTZ only: $T_{MIN} - T_{MAX}$			2.6	mV
Input Offset Voltage Drift	AD8065WARTZ only: $T_{MIN} - T_{MAX}$		1	17	$\mu\text{V}/^\circ\text{C}$
	SOIC package			17	$\mu\text{V}/^\circ\text{C}$
Input Bias Current	$T_{MIN}$ to $T_{MAX}$		2	6	pA
			25	125	pA
Input Offset Current	$T_{MIN}$ to $T_{MAX}$		1	10	pA
				125	pA
Open-Loop Gain	$V_O = \pm 3$ V, $R_L = 1$ k $\Omega$	100	113		dB
	AD8065WARTZ only: $T_{MIN} - T_{MAX}$	100			dB
<b>INPUT CHARACTERISTICS</b>					
Common-Mode Input Impedance			1000    2.1		G $\Omega$    pF
Differential Input Impedance			1000    4.5		G $\Omega$    pF
Input Common-Mode Voltage Range		–5 to +1.7	–5.0 to +2.4		V
FET Input Range	AD8065WARTZ only: $T_{MIN} - T_{MAX}$	–5 to +1.7			V
Common-Mode Rejection Ratio	$V_{CM} = -1$ V to $+1$ V	–85	–100		dB
	$V_{CM} = -1$ V to $+1$ V (SOT-23)	–82	–91		dB
	AD8065WARTZ only: $T_{MIN} - T_{MAX}$	–82			dB

Parameter	Conditions	Min	Typ	Max	Unit
OUTPUT CHARACTERISTICS					
Output Voltage Swing	$R_L = 1\text{ k}\Omega$	-4.88 to +4.90	-4.94 to +4.95		V
	AD8065WARTZ only: $T_{\text{MIN}} - T_{\text{MAX}}$	-4.88 to +4.90			V
Output Current	$R_L = 150\ \Omega$		-4.8 to +4.7		V
	$V_o = 9\text{ V p-p}$ , SFDR $\geq -60\text{ dBc}$ , $f = 500\text{ kHz}$		35		mA
Short-Circuit Current			90		mA
Capacitive Load Drive	30% overshoot $G = +1$		20		pF
POWER SUPPLY					
Operating Range		5		24	V
	AD8065WARTZ only: $T_{\text{MIN}} - T_{\text{MAX}}$	5		10	V
Quiescent Current per Amplifier			6.4	7.2	mA
	AD8065WARTZ only: $T_{\text{MIN}} - T_{\text{MAX}}$			7.2	mA
Power Supply Rejection Ratio	$\pm\text{PSRR}$	-85	-100		dB
	AD8065WARTZ only: $T_{\text{MIN}} - T_{\text{MAX}}$	-85			dB

SPECIFICATIONS  $\pm 12$  V

@  $T_A = 25^\circ\text{C}$ ,  $V_S = \pm 12$  V,  $R_L = 1$  k $\Omega$ , unless otherwise noted.

Table 2.

Parameter	Conditions	Min	Typ	Max	Unit
<b>DYNAMIC PERFORMANCE</b>					
–3 dB Bandwidth	$G = +1$ , $V_o = 0.2$ V p-p (AD8065)	100	145		MHz
	$G = +1$ , $V_o = 0.2$ V p-p (AD8066)	100	115		MHz
	$G = +2$ , $V_o = 0.2$ V p-p		50		MHz
	$G = +2$ , $V_o = 2$ V p-p		40		MHz
	$G = +2$ , $V_o = 0.2$ V p-p		7		MHz
Bandwidth for 0.1 dB Flatness	$G = +2$ , $V_o = 0.2$ V p-p		7		MHz
Input Overdrive Recovery	$G = +1$ , $-12.5$ V to $+12.5$ V		175		ns
Output Overdrive Recovery	$G = -1$ , $-12.5$ V to $+12.5$ V		170		ns
Slew Rate	$G = +2$ , $V_o = 4$ V step	130	180		V/ $\mu$ s
Settling Time to 0.1%	$G = +2$ , $V_o = 2$ V step		55		ns
	$G = +2$ , $V_o = 10$ V step		250		ns
<b>NOISE/HARMONIC PERFORMANCE</b>					
SFDR	$f_c = 1$ MHz, $G = +2$ , $V_o = 2$ V p-p		–100		dBc
	$f_c = 5$ MHz, $G = +2$ , $V_o = 2$ V p-p		–67		dBc
	$f_c = 1$ MHz, $G = +2$ , $V_o = 10$ V p-p		–85		dBc
Third-Order Intercept	$f_c = 10$ MHz, $R_L = 100$ $\Omega$		24		dBm
Input Voltage Noise	$f = 10$ kHz		7		nV/ $\sqrt{\text{Hz}}$
Input Current Noise	$f = 10$ kHz		1		fA/ $\sqrt{\text{Hz}}$
Differential Gain Error	NTSC, $G = +2$ , $R_L = 150$ $\Omega$		0.04		%
Differential Phase Error	NTSC, $G = +2$ , $R_L = 150$ $\Omega$		0.03		Degrees
<b>DC PERFORMANCE</b>					
Input Offset Voltage	$V_{CM} = 0$ V, SOIC package		0.4	1.5	mV
Input Offset Voltage Drift			1	17	$\mu\text{V}/^\circ\text{C}$
Input Bias Current	SOIC package		3	7	pA
	$T_{MIN}$ to $T_{MAX}$		25		pA
Input Offset Current			2	10	pA
	$T_{MIN}$ to $T_{MAX}$		2		pA
Open-Loop Gain	$V_o = \pm 10$ V, $R_L = 1$ k $\Omega$	103	114		dB
<b>INPUT CHARACTERISTICS</b>					
Common-Mode Input Impedance			1000    2.1		G $\Omega$    pF
Differential Input Impedance			1000    4.5		G $\Omega$    pF
Input Common-Mode Voltage Range		–12 to +8.5	–12.0 to +9.5		V
FET Input Range					V
Common-Mode Rejection Ratio	$V_{CM} = -1$ V to $+1$ V	–85	–100		dB
	$V_{CM} = -1$ V to $+1$ V (SOT-23)	–82	–91		dB
<b>OUTPUT CHARACTERISTICS</b>					
Output Voltage Swing	$R_L = 1$ k $\Omega$	–11.8 to +11.8	–11.9 to +11.9		V
	$R_L = 350$ $\Omega$		–11.25 to +11.5		V
Output Current	$V_o = 22$ V p-p, SFDR $\geq -60$ dBc, $f = 500$ kHz		30		mA
Short-Circuit Current			120		mA
Capacitive Load Drive	30% overshoot $G = +1$		25		pF
<b>POWER SUPPLY</b>					
Operating Range		5		24	V
Quiescent Current per Amplifier			6.6	7.4	mA
Power Supply Rejection Ratio	$\pm\text{PSRR}$	–84	–93		dB

## SPECIFICATIONS +5 V

@  $T_A = 25^\circ\text{C}$ ,  $V_S = 5\text{ V}$ ,  $R_L = 1\text{ k}\Omega$ , unless otherwise noted.

Table 3.

Parameter	Conditions	Min	Typ	Max	Unit
<b>DYNAMIC PERFORMANCE</b>					
-3 dB Bandwidth	$G = +1$ , $V_O = 0.2\text{ V p-p}$ (AD8065)	125	155		MHz
	AD8065WARTZ only: $T_{\text{MIN}} - T_{\text{MAX}}$	90			MHz
Bandwidth for 0.1 dB Flatness	$G = +1$ , $V_O = 0.2\text{ V p-p}$ (AD8066)	110	130		MHz
	$G = +2$ , $V_O = 0.2\text{ V p-p}$		50		MHz
Input Overdrive Recovery Time	$G = +2$ , $V_O = 2\text{ V p-p}$		43		MHz
	$G = +2$ , $V_O = 0.2\text{ V p-p}$		6		MHz
Output Recovery Time	$G = +1$ , $-0.5\text{ V to }+5.5\text{ V}$		175		ns
Slew Rate	$G = -1$ , $-0.5\text{ V to }+5.5\text{ V}$		170		ns
	$G = +2$ , $V_O = 2\text{ V step}$	105	160		V/ $\mu\text{s}$
Settling Time to 0.1%	AD8065WARTZ only: $T_{\text{MIN}} - T_{\text{MAX}}$	123			V/ $\mu\text{s}$
	$G = +2$ , $V_O = 2\text{ V step}$		60		ns
<b>NOISE/HARMONIC PERFORMANCE</b>					
SFDR	$f_c = 1\text{ MHz}$ , $G = +2$ , $V_O = 2\text{ V p-p}$		-65		dBc
	$f_c = 5\text{ MHz}$ , $G = +2$ , $V_O = 2\text{ V p-p}$		-50		dBc
Third-Order Intercept	$f_c = 10\text{ MHz}$ , $R_L = 100\ \Omega$		22		dBm
Input Voltage Noise	$f = 10\text{ kHz}$		7		nV/ $\sqrt{\text{Hz}}$
Input Current Noise	$f = 10\text{ kHz}$		0.6		fA/ $\sqrt{\text{Hz}}$
Differential Gain Error	NTSC, $G = +2$ , $R_L = 150\ \Omega$		0.13		%
Differential Phase Error	NTSC, $G = +2$ , $R_L = 150\ \Omega$		0.16		Degrees
<b>DC PERFORMANCE</b>					
Input Offset Voltage	$V_{\text{CM}} = 1.0\text{ V}$ , SOIC package		0.4	1.5	mV
	AD8065WARTZ only: $T_{\text{MIN}} - T_{\text{MAX}}$			2.6	mV
Input Offset Voltage Drift	AD8065WARTZ only: $T_{\text{MIN}} - T_{\text{MAX}}$		1	17	$\mu\text{V}/^\circ\text{C}$
	SOIC package			17	$\mu\text{V}/^\circ\text{C}$
Input Bias Current	$T_{\text{MIN}}$ to $T_{\text{MAX}}$		1	5	pA
	$T_{\text{MIN}}$ to $T_{\text{MAX}}$		25	125	pA
Input Offset Current	$T_{\text{MIN}}$ to $T_{\text{MAX}}$		1	5	pA
	$T_{\text{MIN}}$ to $T_{\text{MAX}}$		1	125	pA
Open-Loop Gain	$V_O = 1\text{ V to }4\text{ V}$ (AD8065)	100	113		dB
	AD8065WARTZ only: $T_{\text{MIN}} - T_{\text{MAX}}$	100			dB
	$V_O = 1\text{ V to }4\text{ V}$ (AD8066)	90	103		dB
<b>INPUT CHARACTERISTICS</b>					
Common-Mode Input Impedance			1000    2.1		$\text{G}\Omega$    pF
Differential Input Impedance			1000    4.5		$\text{G}\Omega$    pF
Input Common-Mode Voltage Range		0 to 1.7	0 to 2.4		V
FET Input Range	AD8065WARTZ only: $T_{\text{MIN}} - T_{\text{MAX}}$	0 to 1.7			V
Common-Mode Rejection Ratio	$V_{\text{CM}} = 0.5\text{ V to }1.5\text{ V}$	-74	-100		dB
	$V_{\text{CM}} = 1\text{ V to }2\text{ V}$ (SOT-23)	-78	-91		dB
	AD8065WARTZ only: $T_{\text{MIN}} - T_{\text{MAX}}$	-76			dB
<b>OUTPUT CHARACTERISTICS</b>					
Output Voltage Swing	$R_L = 1\text{ k}\Omega$	0.1 to 4.85	0.03 to 4.95		V
	AD8065WARTZ only: $T_{\text{MIN}} - T_{\text{MAX}}$	0.1 to 4.85			V
Output Current	$R_L = 150\ \Omega$		0.07 to 4.83		V
Short-Circuit Current	$V_O = 4\text{ V p-p}$ , SFDR $\geq -60\text{ dBc}$ , $f = 500\text{ kHz}$		35		mA
Capacitive Load Drive	30% overshoot $G = +1$		75		mA
			5		pF

Parameter	Conditions	Min	Typ	Max	Unit
POWER SUPPLY					
Operating Range		5		24	V
Quiescent Current per Amplifier	AD8065WARTZ only: $T_{MIN} - T_{MAX}$	5		10	V
		5.8	6.4	7.0	mA
Power Supply Rejection Ratio	AD8065WARTZ only: $T_{MIN} - T_{MAX}$			7.0	mA
	$\pm$ PSRR	-78	-100		dB
	AD8065WARTZ only: $T_{MIN} - T_{MAX}$	-78			dB



## ABSOLUTE MAXIMUM RATINGS

Table 4.

Parameter	Rating
Supply Voltage	26.4 V
Power Dissipation	See Figure 3
Common-Mode Input Voltage	$V_{EE} - 0.5 \text{ V}$ to $V_{CC} + 0.5 \text{ V}$
Differential Input Voltage	1.8 V
Storage Temperature Range	$-65^{\circ}\text{C}$ to $+125^{\circ}\text{C}$
Operating Temperature Range	$-40^{\circ}\text{C}$ to $+85^{\circ}\text{C}$
AD8065WARTZ Only	$-40^{\circ}\text{C}$ to $+105^{\circ}\text{C}$
Lead Temperature (Soldering, 10 sec)	$300^{\circ}\text{C}$

Stresses at or above those listed under Absolute Maximum Ratings may cause permanent damage to the product. This is a stress rating only; functional operation of the product at these or any other conditions above those indicated in the operational section of this specification is not implied. Operation beyond the maximum operating conditions for extended periods may affect product reliability.

### MAXIMUM POWER DISSIPATION

The maximum safe power dissipation in the AD8065/AD8066 packages is limited by the associated rise in junction temperature ( $T_J$ ) on the die. The plastic encapsulating the die locally reaches the junction temperature. At approximately  $150^{\circ}\text{C}$ , which is the glass transition temperature, the plastic changes its properties. Even temporarily exceeding this temperature limit can change the stresses that the package exerts on the die, permanently shifting the parametric performance of the AD8065/AD8066. Exceeding a junction temperature of  $175^{\circ}\text{C}$  for an extended time can result in changes in the silicon devices, potentially causing failure.

The still air thermal properties of the package and PCB ( $\theta_{JA}$ ), ambient temperature ( $T_A$ ), and total power dissipated in the package ( $P_D$ ) determine the junction temperature of the die. The junction temperature can be calculated by

$$T_J = T_A + (P_D \times \theta_{JA})$$

The power dissipated in the package ( $P_D$ ) is the sum of the quiescent power dissipation and the power dissipated in the package due to the load drive for all outputs. The quiescent power is the voltage between the supply pins ( $V_S$ ) times the quiescent current ( $I_S$ ). Assuming the load ( $R_L$ ) is referenced to midsupply, then the total drive power is  $V_S / 2 \times I_{OUT}$ , some of which is dissipated in the package and some in the load ( $V_{OUT} \times I_{OUT}$ ). The difference between the total drive power and the load power is the drive power dissipated in the package.

$$P_D = \text{Quiescent Power} + (\text{Total Drive Power} - \text{Load Power})$$

$$P_D = (V_S \times I_S) + \left( \frac{V_S}{2} \times \frac{V_{OUT}}{R_L} \right) - \frac{V_{OUT}^2}{R_L}$$

RMS output voltages should be considered. If  $R_L$  is referenced to  $V_{S-}$ , as in single-supply operation, then the total drive power is  $V_S \times I_{OUT}$ .

If the rms signal levels are indeterminate, then consider the worst case, when  $V_{OUT} = V_S/4$  for  $R_L$  to midsupply.

$$P_D = (V_S \times I_S) + \frac{(V_S/4)^2}{R_L}$$

In single-supply operation with  $R_L$  referenced to  $V_{S-}$ , worst case is  $V_{OUT} = V_S/2$ .

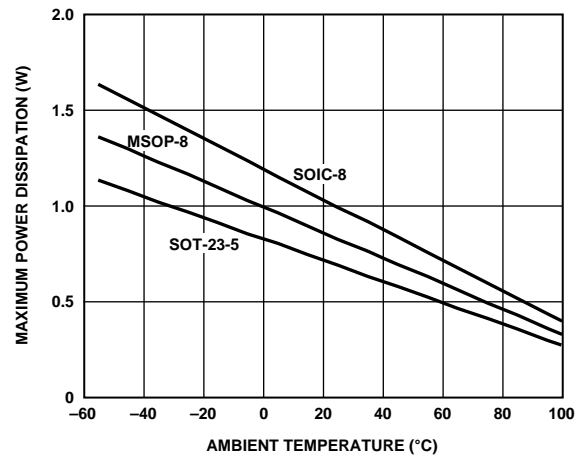


Figure 3. Maximum Power Dissipation vs. Temperature for a 4-Layer Board

Airflow increases heat dissipation, effectively reducing  $\theta_{JA}$ . Also, more metal directly in contact with the package leads from metal traces, through holes, ground, and power planes reduce the  $\theta_{JA}$ . Care must be taken to minimize parasitic capacitances at the input leads of high speed op amps as discussed in the Layout, Grounding, and Bypassing Considerations section.

Figure 3 shows the maximum safe power dissipation in the package vs. the ambient temperature for the SOIC ( $125^{\circ}\text{C}/\text{W}$ ), SOT-23 ( $180^{\circ}\text{C}/\text{W}$ ), and MSOP ( $150^{\circ}\text{C}/\text{W}$ ) packages on a JEDEC standard 4-layer board.  $\theta_{JA}$  values are approximations.

### OUTPUT SHORT CIRCUIT

Shorting the output to ground or drawing excessive current for the AD8065/AD8066 will likely cause catastrophic failure.

### ESD CAUTION



**ESD (electrostatic discharge) sensitive device.** Charged devices and circuit boards can discharge without detection. Although this product features patented or proprietary protection circuitry, damage may occur on devices subjected to high energy ESD. Therefore, proper ESD precautions should be taken to avoid performance degradation or loss of functionality.

# TYPICAL PERFORMANCE CHARACTERISTICS

Default Conditions:  $\pm 5\text{ V}$ ,  $C_L = 5\text{ pF}$ ,  $R_L = 1\text{ k}\Omega$ ,  $V_{OUT} = 2\text{ V p-p}$ , Temperature =  $25^\circ\text{C}$ .



Figure 4. Small Signal Frequency Response for Various Gains

02916-E-004

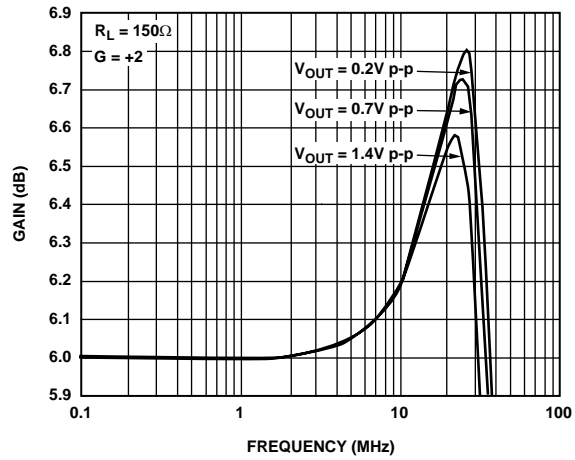


Figure 7. 0.1 dB Flatness Frequency Response (See Figure 43)

02916-E-007

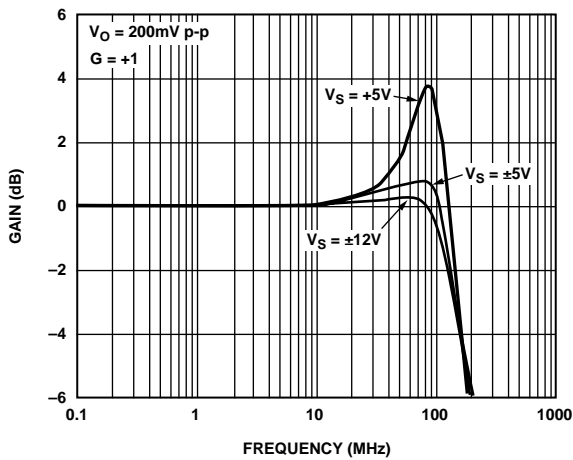


Figure 5. Small Signal Frequency Response for Various Supplies (See Figure 42)

02916-E-005

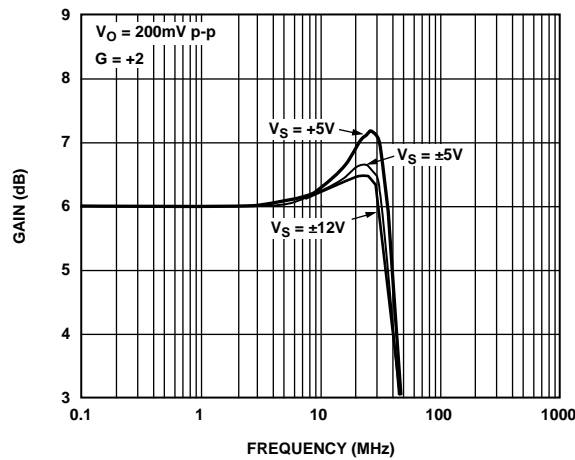


Figure 8. Small Signal Frequency Response for Various Supplies (See Figure 43)

02916-E-008

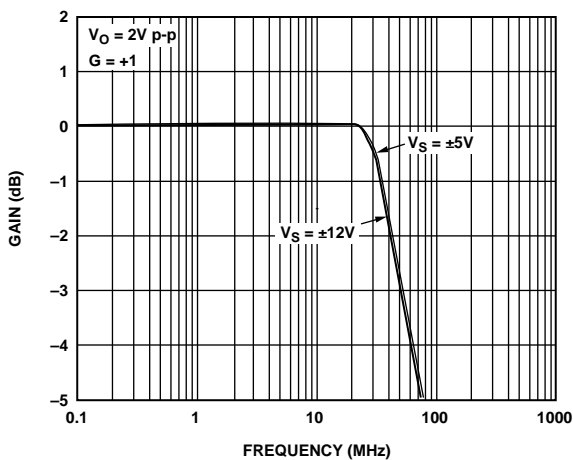


Figure 6. Large Signal Frequency Response for Various Supplies (See Figure 42)

02916-E-006

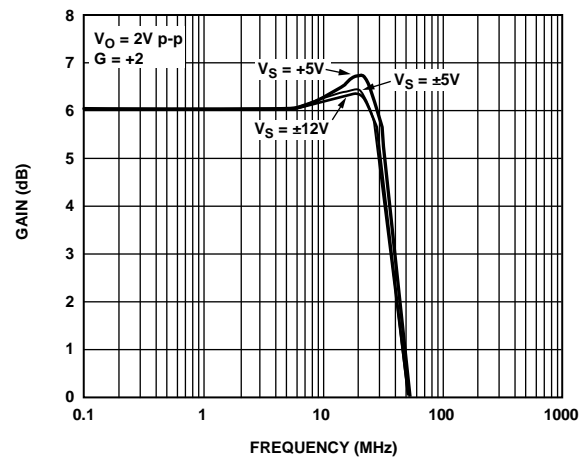


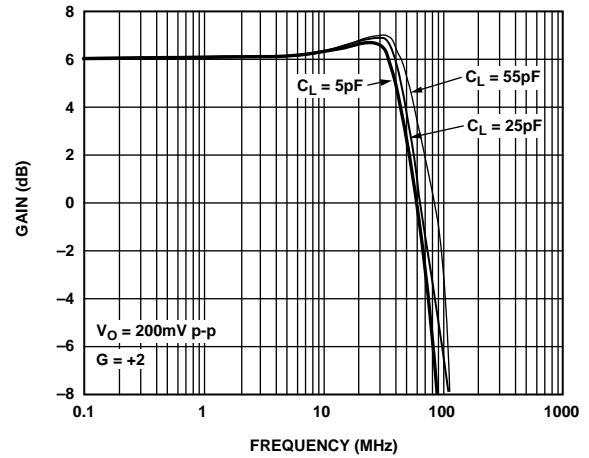
Figure 9. Large Signal Frequency Response for Various Supplies (See Figure 43)

02916-E-009



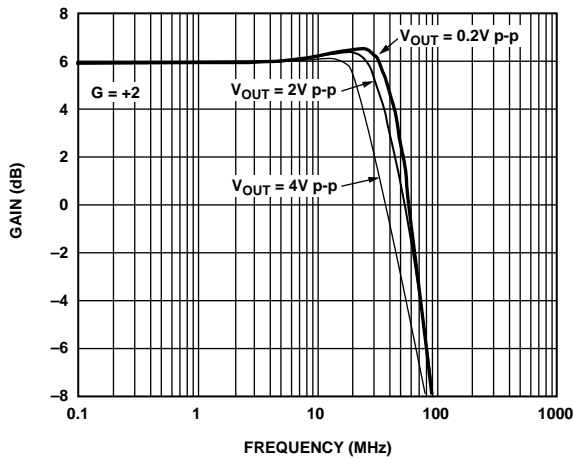
02916E-010

Figure 10. Small Signal Frequency Response for Various  $C_{LOAD}$  (See Figure 42)



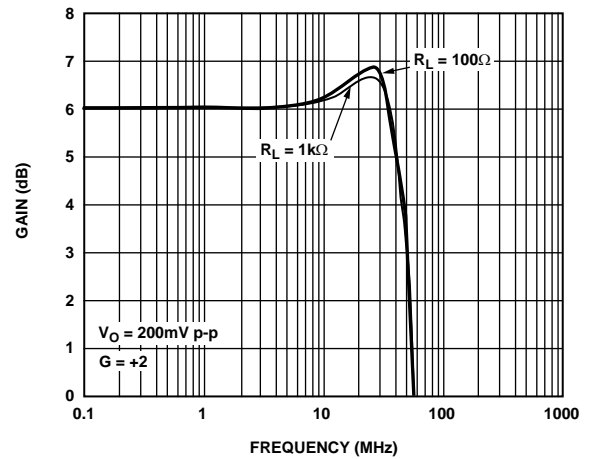
02916E-013

Figure 13. Small Signal Frequency Response for Various  $C_{LOAD}$  (See Figure 43)



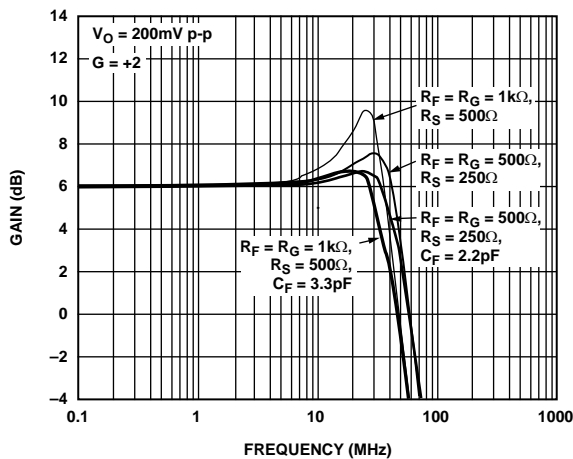
02916E-011

Figure 11. Frequency Response for Various Output Amplitudes (See Figure 43)



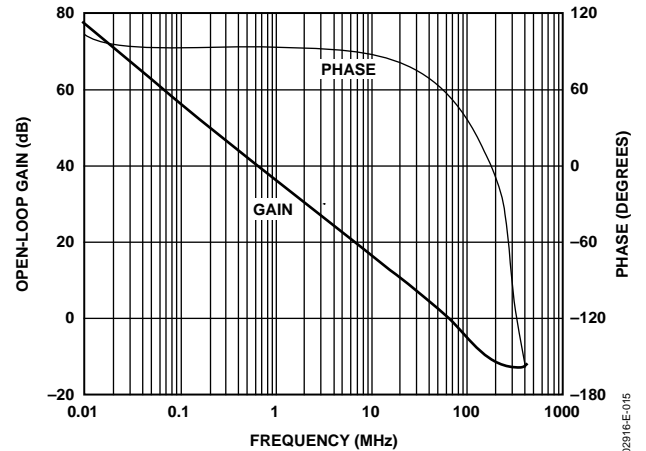
02916E-014

Figure 14. Small Signal Frequency Response for Various  $R_{LOAD}$  (See Figure 43)



02916E-012

Figure 12. Small Signal Frequency Response for Various  $R_F/C_F$  (See Figure 43)



02916E-015

Figure 15. Open-Loop Response



Figure 16. Harmonic Distortion vs. Frequency for Various Loads (See Figure 43)

02916-E-016



Figure 19. Harmonic Distortion vs. Frequency for Various Gains (See Figure 42 and Figure 43)

02916-E-019



Figure 17. Harmonic Distortion vs. Amplitude for Various Loads  $V_S = \pm 12V$  (See Figure 43)

02916-E-017



Figure 20. Harmonic Distortion vs. Frequency for Various Amplitudes (See Figure 43)

02916-E-020



Figure 18. Third-Order Intercept vs. Frequency and Supply Voltage

02916-E-018



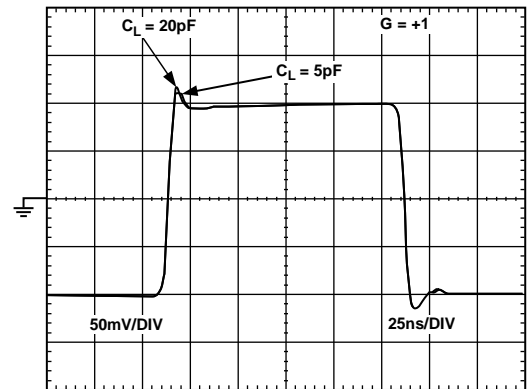
Figure 21. Voltage Noise

02916-E-021



02916-022

Figure 22. Small Signal Transient Response 5 V Supply (See Figure 42)



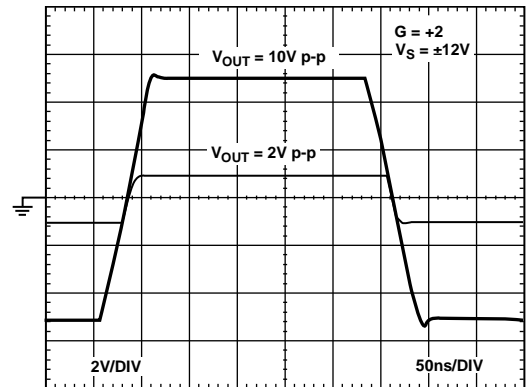
02916-025

Figure 25. Small Signal Transient Response  $\pm 5$  V (See Figure 42)



02916-023

Figure 23. Large Signal Transient Response (See Figure 42)



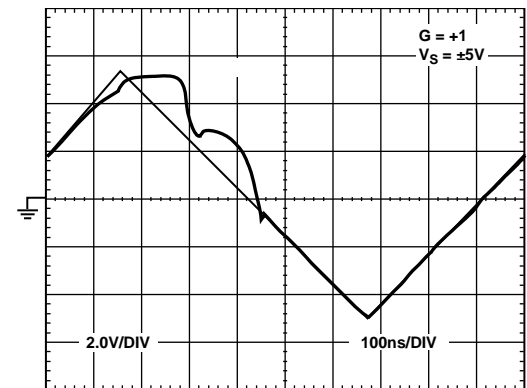
02916-026

Figure 26. Large Signal Transient Response (See Figure 43)



02916-024

Figure 24. Output Overdrive Recovery (See Figure 44)



02916-027

Figure 27. Input Overdrive Recovery (See Figure 42)



Figure 28. Long-Term Settling Time (See Figure 49)

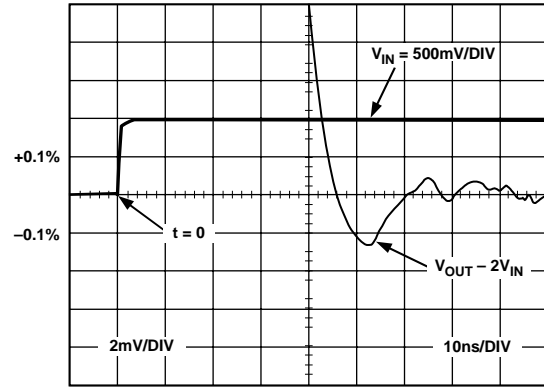


Figure 31. 0.1% Short-Term Settling Time (See Figure 49)

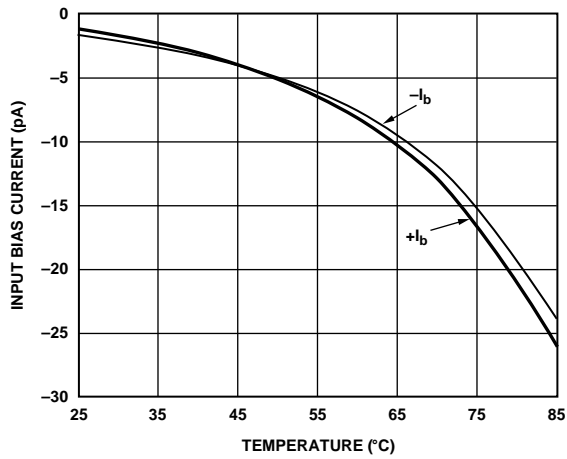


Figure 29. Input Bias Current vs. Temperature

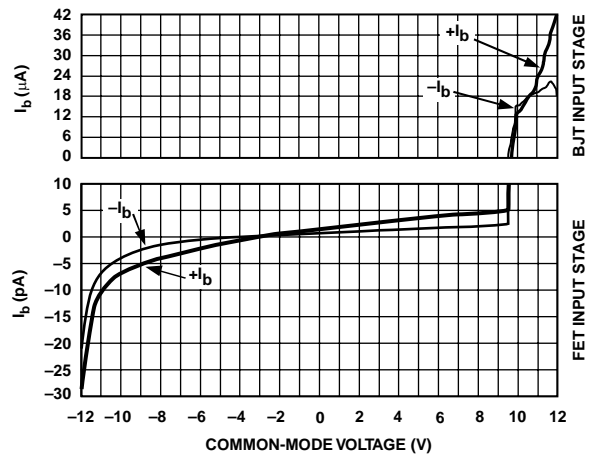


Figure 32. Input Bias Current vs. Common-Mode Voltage Range (See the Input and Output Overload Behavior Section)

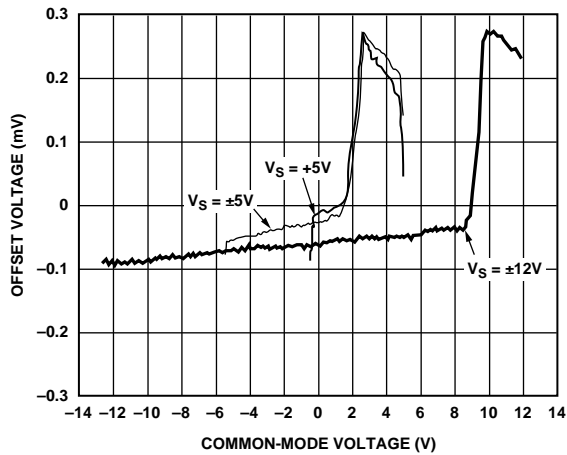


Figure 30. Input Offset Voltage vs. Common-Mode Voltage

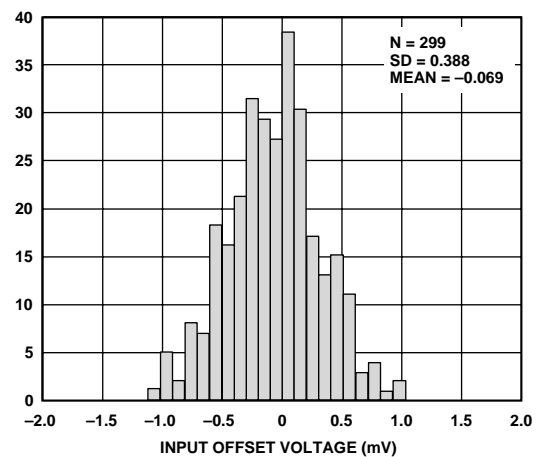


Figure 33. Input Offset Voltage

02916-E-028

02916-E-031

02916-E-029

02916-E-032

02916-E-030

02916-E-033

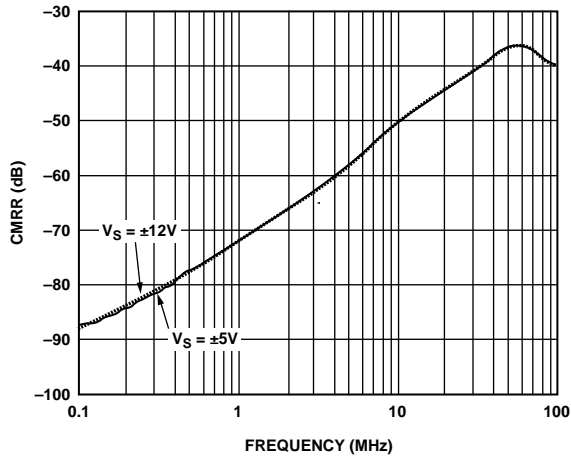


Figure 34. CMRR vs. Frequency (See Figure 46)

02916-E-034

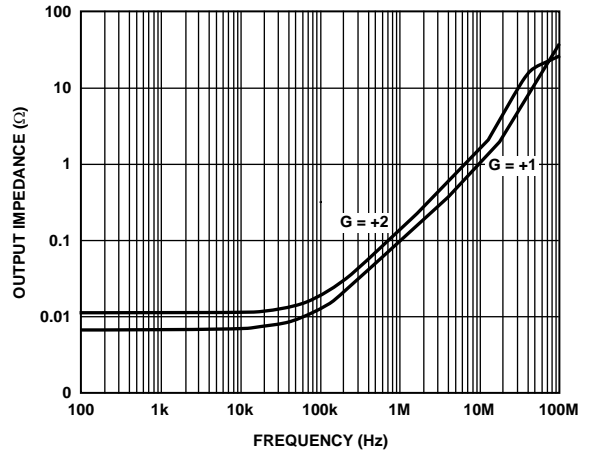


Figure 37. Output Impedance vs. Frequency (See Figure 45 and Figure 47)

02916-E-037

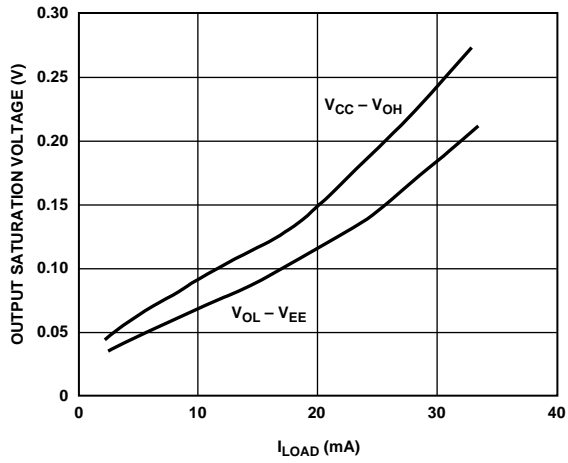


Figure 35. Output Saturation Voltage vs. Output Load Current

02916-E-035

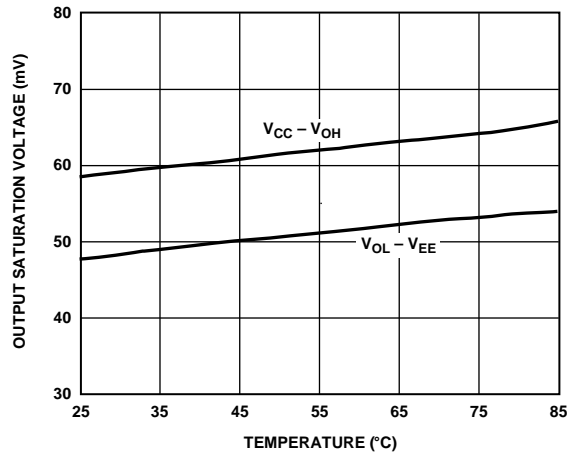


Figure 38. Output Saturation Voltage vs. Temperature

02916-E-038

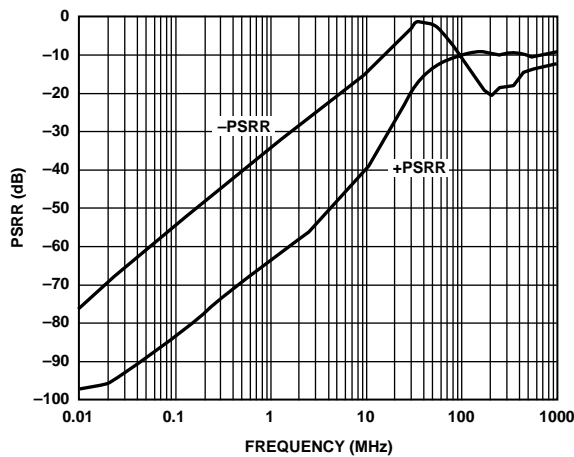


Figure 36. PSRR vs. Frequency (See Figure 48 and Figure 50)

02916-E-036

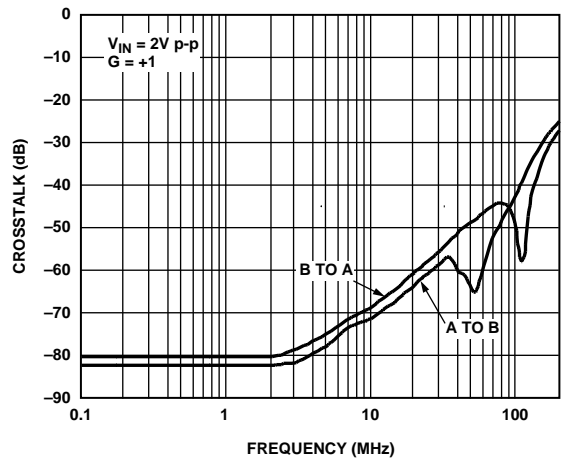
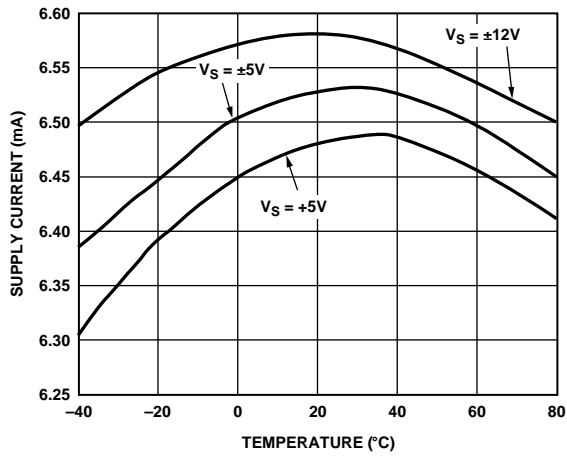


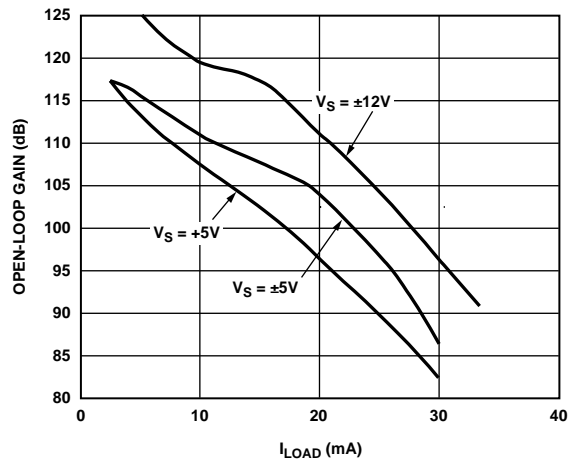
Figure 39. Crosstalk vs. Frequency (See Figure 51)

02916-E-039



02816E-040

Figure 40. Quiescent Supply Current vs. Temperature for Various Supply Voltages



02816E-041

Figure 41. Open-Loop Gain vs. Load Current for Various Supply Voltages



# TEST CIRCUITS

## SOIC-8 Pinout

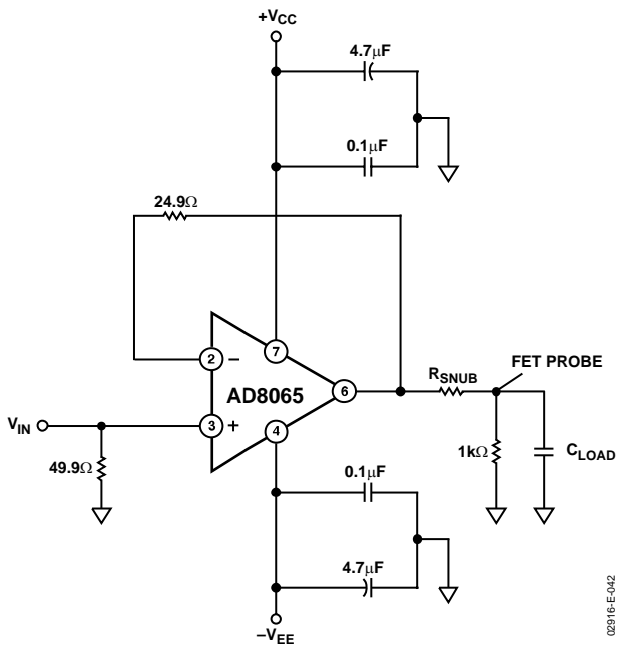


Figure 42.  $G = +1$

02916E-042

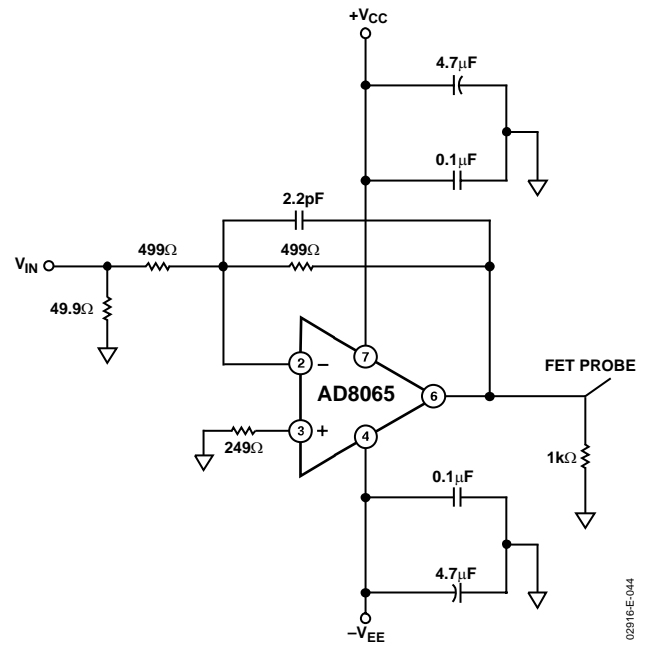


Figure 44.  $G = -1$

02916E-044

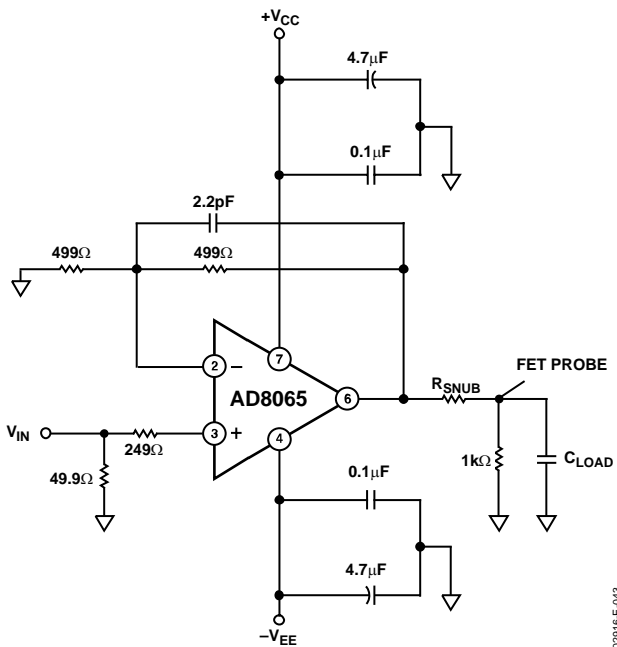


Figure 43.  $G = +2$

02916E-043

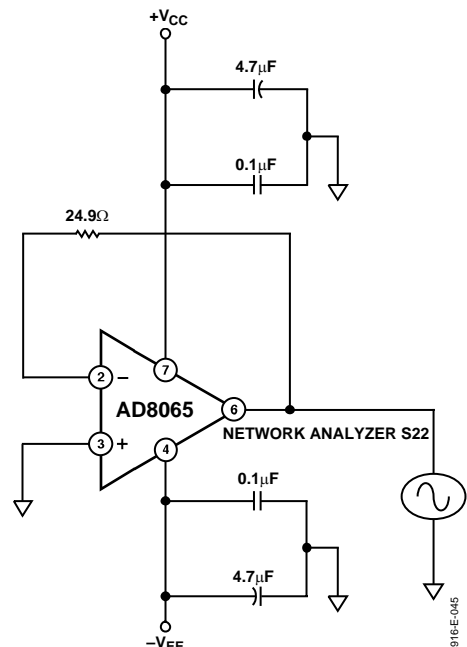


Figure 45. Output Impedance  $G = +1$

02916E-045



Figure 46. CMRR

02916-E-046



Figure 48. Positive PSRR

02916-E-048



Figure 47. Output Impedance  $G = +2$

02916-E-047



Figure 49. Settling Time

02916-E-049

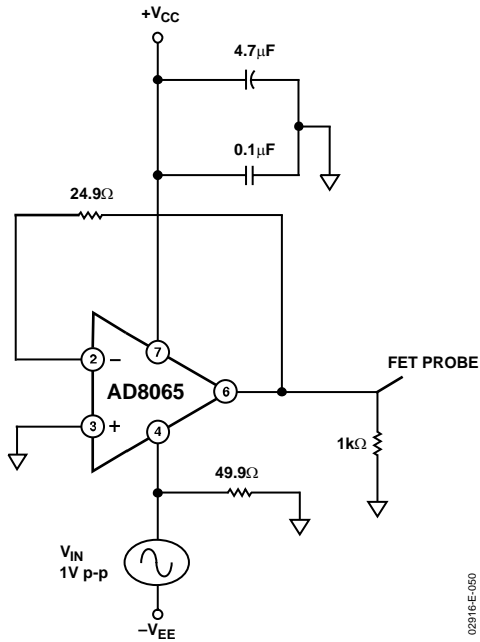


Figure 50. Negative PSRR

02916-E-050



Figure 52. Single Supply

02916-E-052

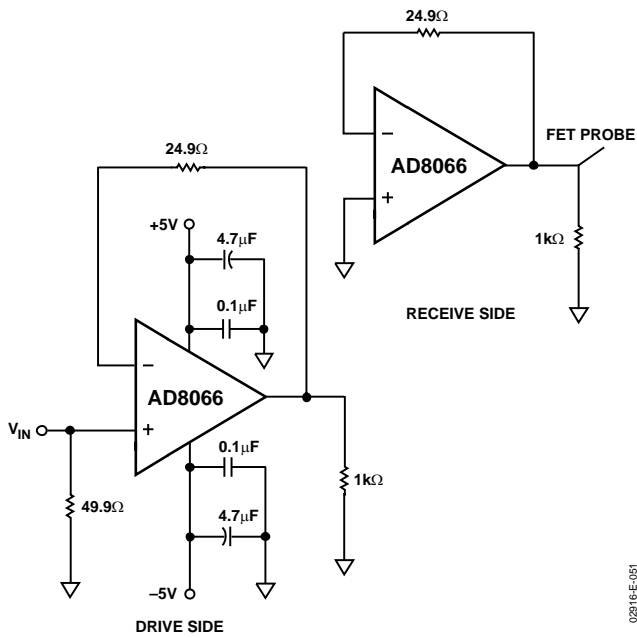


Figure 51. Crosstalk—AD8066

02916-E-051

## THEORY OF OPERATION

The AD8065/AD8066 are voltage feedback operational amplifiers that combine a laser-trimmed JFET input stage with the Analog Devices eXtra Fast Complementary Bipolar (XFCB) process, resulting in an outstanding combination of precision and speed. The supply voltage range is from 5 V to 24 V. The amplifiers feature a patented rail-to-rail output stage capable of driving within 0.5 V of either power supply while sourcing or sinking up to 30 mA. Also featured is a single-supply input stage that handles common-mode signals from below the negative supply to within 3 V of the positive rail. Operation beyond the JFET input range is possible because of an auxiliary bipolar input stage that functions with input voltages up to the positive supply. The amplifiers operate as if they have a rail-to-rail input and exhibit no phase reversal behavior for common-mode voltages within the power supply.

With voltage noise of 7 nV/√Hz and -88 dBc distortion for 1 MHz, 2 V p-p signals, the AD8065/AD8066 are a great choice for high resolution data acquisition systems. Their low noise, sub-pA input current, precision offset, and high speed make them superb preamps for fast photodiode applications. The speed and output drive capability of the AD8065/AD8066 also make them useful in video applications.

### CLOSED-LOOP FREQUENCY RESPONSE

The AD8065/AD8066 are classic voltage feedback amplifiers with an open-loop frequency response that can be approximated as the integrator response shown in Figure 53. Basic closed-loop frequency response for inverting and noninverting configurations can be derived from the schematics shown.

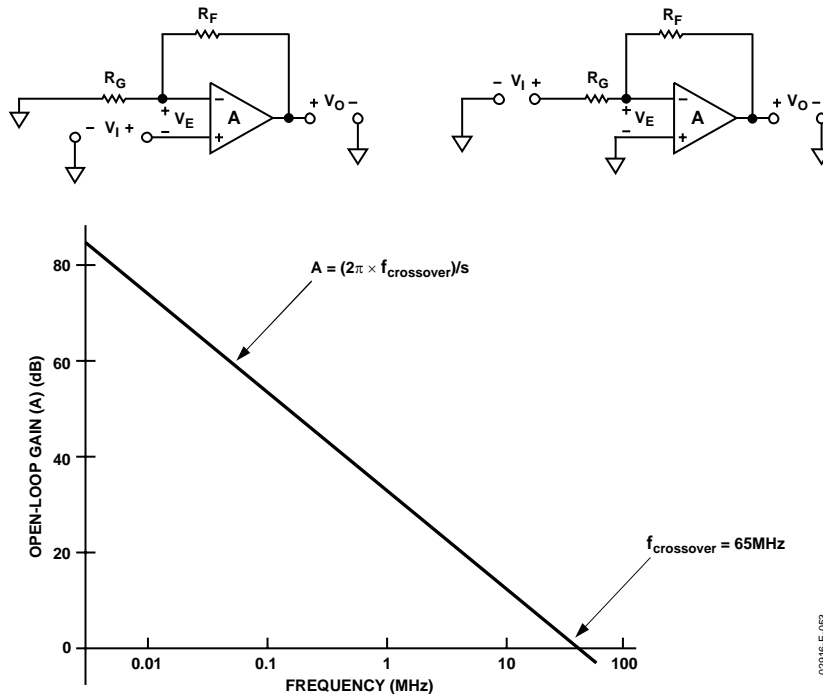


Figure 53. Open-Loop Gain vs. Frequency and Basic Connections

### NONINVERTING CLOSED-LOOP FREQUENCY RESPONSE

Solving for the transfer function

$$\frac{V_O}{V_I} = \frac{2\pi \times f_{crossover} (R_G + R_F)}{(R_F + R_G)s + 2\pi \times f_{crossover} \times R_G}$$

where  $f_{crossover}$  is the frequency where the amplifier's open-loop gain equals 0 db

At dc  $\frac{V_O}{V_I} = \frac{R_F + R_G}{R_G}$

Closed-loop -3 dB frequency

$$f_{-3dB} = f_{crossover} \times \frac{R_G}{R_F + R_G}$$

### INVERTING CLOSED-LOOP FREQUENCY RESPONSE

$$\frac{V_O}{V_I} = \frac{-2\pi \times f_{crossover} \times R_F}{s(R_F + R_G) + 2\pi \times f_{crossover} \times R_G}$$

At dc  $\frac{V_O}{V_I} = -\frac{R_F}{R_G}$

Closed-loop -3 dB frequency

$$f_{-3dB} = f_{crossover} \times \frac{R_G}{R_F + R_G}$$

The closed-loop bandwidth is inversely proportional to the noise gain of the op amp circuit,  $(R_F + R_G)/R_G$ . This simple model is accurate for noise gains above 2. The actual bandwidth of circuits with noise gains at or below 2 is higher than those predicted with this model due to the influence of other poles in the frequency response of the real op amp.



Figure 54. Voltage Feedback Amplifier DC Errors

Figure 54 shows a voltage feedback amplifier’s dc errors. For both inverting and noninverting configurations

$$V_O (error) = I_{b+} \times R_S \left( \frac{R_G + R_F}{R_G} \right) - I_{b-} \times R_F + V_{OS} \left( \frac{R_G + R_F}{R_G} \right)$$

The voltage error due to  $I_{b+}$  and  $I_{b-}$  is minimized if  $R_S = R_F \parallel R_G$  (though with the AD8065 input currents at typically less than 20 pA over temperature, this is likely not a concern). To include common-mode and power supply rejection effects, total  $V_{OS}$  can be modeled

$$V_{OS} = V_{OSnom} + \frac{\Delta V_S}{PSR} + \frac{\Delta V_{CM}}{CMR}$$

$V_{OSnom}$  is the offset voltage specified at nominal conditions,  $\Delta V_S$  is the change in power supply from nominal conditions, PSR is the power supply rejection,  $\Delta V_{CM}$  is the change in common-mode voltage from nominal conditions, and CMR is the common-mode rejection.

**WIDEBAND OPERATION**

Figure 42 through Figure 44 show the circuits used for wideband characterization for gains of +1, +2, and -1. Source impedance at the summing junction ( $R_F \parallel R_G$ ) forms a pole in the amplifier’s loop response with the amplifier’s input capacitance of 6.6 pF. This can cause peaking and ringing if the time constant formed is too low. Feedback resistances of 300 Ω to 1 kΩ are recommended, because they do not unduly load down the amplifier, and the time constant formed will not be too low. Peaking in the frequency response can be compensated for with a small capacitor ( $C_F$ ) in parallel with the feedback resistor, as illustrated in Figure 12. This shows the effect of different feedback capacitances on the peaking and bandwidth for a noninverting  $G = +2$  amplifier.

For the best settling times and the best distortion, the impedances at the AD8065/AD8066 input terminals should be matched. This minimizes nonlinear common-mode capacitive effects that can degrade ac performance.

Actual distortion performance depends on a number of variables:

- The closed-loop gain of the application
- Whether it is inverting or noninverting
- Amplifier loading
- Signal frequency and amplitude
- Board layout

Also see Figure 16 to Figure 20. The lowest distortion is obtained with the AD8065 used in low gain inverting applications, because this eliminates common-mode effects. Higher closed-loop gains result in worse distortion performance.

**INPUT PROTECTION**

The inputs of the AD8065/AD8066 are protected with back-to-back diodes between the input terminals as well as ESD diodes to either power supply. This results in an input stage with picoamps of input current that can withstand up to 1500 V ESD events (human body model) with no degradation.

Excessive power dissipation through the protection devices destroys or degrades the performance of the amplifier. Differential voltages greater than 0.7 V result in an input current of approximately  $(|V_+ - V_-| - 0.7 \text{ V})/R_I$ , where  $R_I$  is the resistance in series with the inputs.

For input voltages beyond the positive supply, the input current is approximately  $(V_I - V_{CC} - 0.7)/R_I$ . Beyond the negative supply, the input current is about  $(V_I - V_{EE} + 0.7)/R_I$ . If the inputs of the amplifier are to be subjected to sustained differential voltages greater than 0.7 V, or to input voltages beyond the amplifier power supply, input current should be limited to 30 mA by an appropriately sized input resistor ( $R_I$ ), as shown in Figure 55.

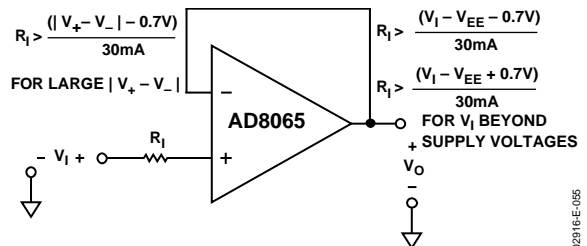


Figure 55. Current-Limiting Resistor

## THERMAL CONSIDERATIONS

With 24 V power supplies and 6.5 mA quiescent current, the AD8065 dissipates 156 mW with no load. The AD8066 dissipates 312 mW. This can lead to noticeable thermal effects, especially in the small SOT-23-5 (thermal resistance of  $160^{\circ}\text{C}/\text{W}$ ).  $V_{OS}$  temperature drift is trimmed to guarantee a maximum drift of  $17\ \mu\text{V}/^{\circ}\text{C}$ , so it can change up to 0.425 mV due to warm-up effects for an AD8065/AD8066 in a SOT-23-5 package on 24 V.

$I_b$  increases by a factor of 1.7 for every  $10^{\circ}\text{C}$  rise in temperature.  $I_b$  is close to five times higher at 24 V supplies as opposed to a single 5 V supply.

Heavy loads increase power dissipation and raise the chip junction temperature as described in the Maximum Power Dissipation section. Care should be taken not to exceed the rated power dissipation of the package.

## INPUT AND OUTPUT OVERLOAD BEHAVIOR

A simplified schematic of the AD8065/AD8066 input stage is shown in Figure 56. This shows the cascoded N-channel JFET input pair, the ESD and other protection diodes, and the auxiliary NPN input stage that eliminates any phase inversion behavior. When the common-mode input voltage to the amplifier is driven to within approximately 3 V of the positive power supply, the input JFET's bias current turns off and the bias of the NPN pair turns on, taking over control of the amplifier. The NPN differential pair now sets the amplifier's offset, and the input bias current is now in the range of several tens of microamps. This behavior is shown in Figure 32. Normal operation resumes when the common-mode voltage goes below the 3 V from the positive supply threshold.

The output transistors of the rail-to-rail output stage have circuitry to limit the extent of their saturation when the output is overdriven. This helps output recovery time. Output recovery from a 0.5 V output overdrive on a  $\pm 5\ \text{V}$  supply is shown in Figure 24.

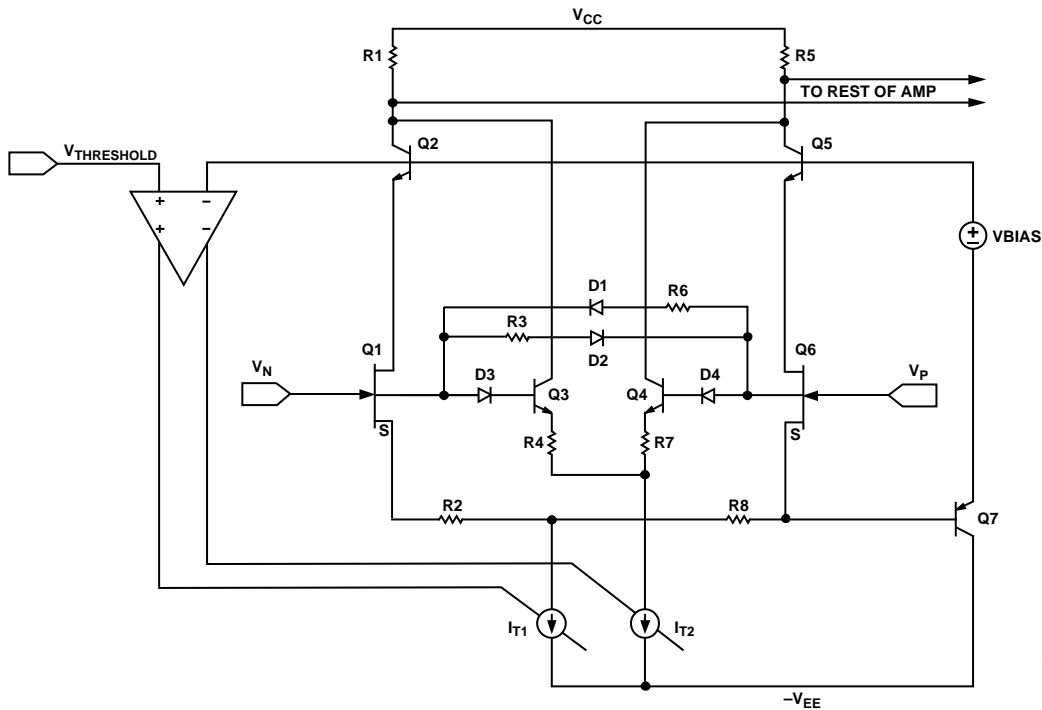


Figure 56. Simplified Input Stage

## LAYOUT, GROUNDING, AND BYPASSING CONSIDERATIONS

### POWER SUPPLY BYPASSING

Power supply pins are actually inputs and care must be taken so that a noise-free stable dc voltage is applied. The purpose of bypass capacitors is to create low impedances from the supply to ground at all frequencies, thereby shunting or filtering most of the noise.

Decoupling schemes are designed to minimize the bypassing impedance at all frequencies with a parallel combination of capacitors. 0.1  $\mu\text{F}$  (X7R or NPO) chip capacitors are critical and should be as close as possible to the amplifier package. The 4.7  $\mu\text{F}$  tantalum capacitor is less critical for high frequency bypassing, and, in most cases, only one is needed per board at the supply inputs.

### GROUNDING

A ground plane layer is important in densely packed PC boards to spread the current minimizing parasitic inductances. However, an understanding of where the current flows in a circuit is critical to implementing effective high speed circuit design. The length of the current path is directly proportional to the magnitude of parasitic inductances and, therefore, the high frequency impedance of the path. High speed currents in an inductive ground return create unwanted voltage noise.

The length of the high frequency bypass capacitor leads is most critical. A parasitic inductance in the bypass grounding works against the low impedance created by the bypass capacitor. Place the ground leads of the bypass capacitors at the same physical location. Because load currents flow from the supplies as well, the ground for the load impedance should be at the same physical location as the bypass capacitor grounds. For the larger value capacitors, which are effective at lower frequencies, the current return path distance is less critical.

### LEAKAGE CURRENTS

Poor PC board layout, contaminants, and the board insulator material can create leakage currents that are much larger than the input bias current of the AD8065/AD8066. Any voltage differential between the inputs and nearby runs sets up leakage currents through the PC board insulator, for example, 1 V/100 G $\Omega$  = 10 pA. Similarly, any contaminants on the board can create significant leakage (skin oils are a common problem). To reduce leakage significantly, put a guard ring (shield) around the inputs and input leads that are driven to the same voltage potential as the inputs. This way there is no voltage potential between the

inputs and surrounding area to set up any leakage currents. For the guard ring to be completely effective, it must be driven by a relatively low impedance source and should completely surround the input leads on all sides, above and below, using a multilayer board.

Another effect that can cause leakage currents is the charge absorption of the insulator material itself. Minimizing the amount of material between the input leads and the guard ring helps to reduce the absorption. Also, low absorption materials, such as Teflon® or ceramic, could be necessary in some instances.

### INPUT CAPACITANCE

Along with bypassing and ground, high speed amplifiers can be sensitive to parasitic capacitance between the inputs and ground. A few pF of capacitance reduces the input impedance at high frequencies, in turn increasing the amplifier's gain, causing peaking of the frequency response or even oscillations, if severe enough. It is recommended that the external passive components connected to the input pins be placed as close as possible to the inputs to avoid parasitic capacitance. The ground and power planes must be kept at a small distance from the input pins on all layers of the board.

### OUTPUT CAPACITANCE

To a lesser extent, parasitic capacitances on the output can cause peaking and ringing of the frequency response. There are two methods to effectively minimize their effect:

- As shown in Figure 57, put a small value resistor ( $R_S$ ) in series with the output to isolate the load capacitor from the amp's output stage. A good value to choose is 20  $\Omega$  (see Figure 10).
- Increase the phase margin with higher noise gains or add a pole with a parallel resistor and capacitor from  $-IN$  to the output.

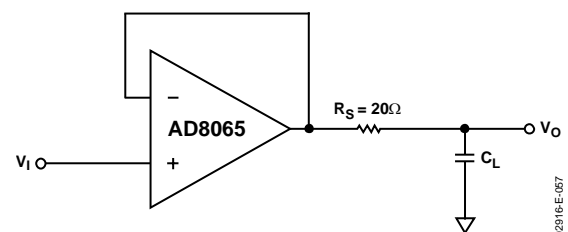


Figure 57. Output Isolation Resistor



Figure 58. Wideband Photodiode Preamp

**INPUT-TO-OUTPUT COUPLING**

To minimize capacitive coupling between the inputs and output, the output signal traces should not be parallel with the inputs.

**WIDEBAND PHOTODIODE PREAMP**

Figure 58 shows an I/V converter with an electrical model of a photodiode. The basic transfer function is

$$V_{OUT} = \frac{I_{PHOTO} \times R_F}{1 + sC_F R_F}$$

where  $I_{PHOTO}$  is the output current of the photodiode, and the parallel combination of  $R_F$  and  $C_F$  sets the signal bandwidth.

The stable bandwidth attainable with this preamp is a function of  $R_F$ , the gain bandwidth product of the amplifier, and the total capacitance at the amplifier’s summing junction, including  $C_S$  and the amplifier input capacitance.  $R_F$  and the total capacitance produce a pole in the amplifier’s loop transmission that can result in peaking and instability. Adding  $C_F$  creates a 0 in the loop transmission that compensates for the pole’s effect and reduces the signal bandwidth. It can be shown that the signal bandwidth resulting in a 45° phase margin ( $f_{(45)}$ ) is defined by

$$f_{(45)} = \sqrt{\frac{f_{CR}}{2\pi \times R_F \times C_S}}$$

where  $f_{CR}$  is the amplifier crossover frequency,  $R_F$  is the feedback resistor, and  $C_S$  is the total capacitance at the amplifier summing junction (amplifier + photodiode + board parasitics).

The value of  $C_F$  that produces  $f_{(45)}$  can be shown to be

$$C_F = \sqrt{\frac{C_S}{2\pi \times R_F \times f_{CR}}}$$

The frequency response in this case shows about 2 dB of peaking and 15% overshoot. Doubling  $C_F$  and cutting the bandwidth in half results in a flat frequency response with about 5% transient overshoot.

The preamp’s output noise over frequency is shown in Figure 59.

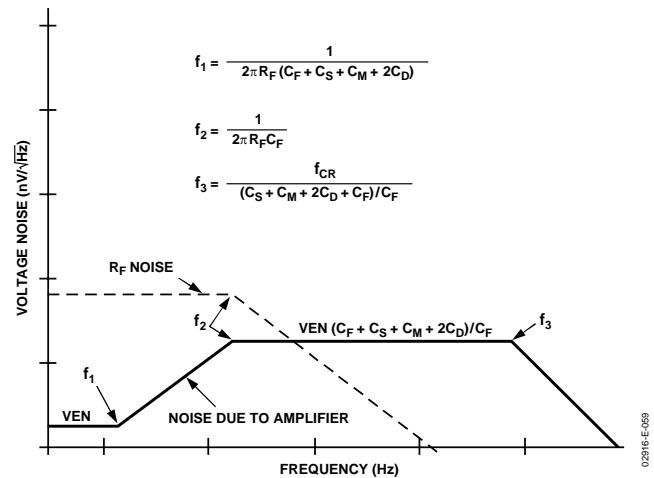


Figure 59. Photodiode Voltage Noise Contributions

The pole in the loop transmission translates to a 0 in the amplifier’s noise gain, leading to an amplification of the input voltage noise over frequency. The loop transmission 0 introduced by  $C_F$  limits the amplification. The noise gain bandwidth extends past the preamp signal bandwidth and is eventually rolled off by the decreasing loop gain of the amplifier. Keeping the input terminal impedances matched is recommended to eliminate common-mode noise peaking effects, which adds to the output noise.

Integrating the square of the output voltage noise spectral density over frequency and then taking the square root allows users to obtain the total rms output noise of the preamp. Table 5 summarizes approximations for the amplifier and feedback and source resistances. Noise components for an example preamp with  $R_F = 50 \text{ k}\Omega$ ,  $C_S = 15 \text{ pF}$ , and  $C_F = 2 \text{ pF}$  (bandwidth of about 1.6 MHz) are also listed.



Table 5. RMS Noise Contributions of Photodiode Preamp

Contributor	Expression	RMS Noise with $R_F = 50\text{ k}\Omega$ , $C_S = 15\text{ pF}$ , $C_F = 2\text{ pF}$
$R_F (\times 2)$	$\sqrt{2 \times 4 kT \times R_F \times f_2 \times 1.57}$	64.5 $\mu\text{V}$
Amp to $f_1$	$VEN \times \sqrt{f_1}$	2.4 $\mu\text{V}$
Amp ( $f_2 - f_1$ )	$VEN \times \sqrt{\frac{C_S + C_M + C_F + 2C_D}{C_F}} \times \sqrt{f_2 - f_1}$	31 $\mu\text{V}$
Amp to (past $f_2$ )	$VEN \times \sqrt{\frac{C_S + C_M + 2C_D + C_F}{C_F}} \times \sqrt{f_3 \times 1.57}$	260 $\mu\text{V}$
		270 $\mu\text{V}$ (Total)

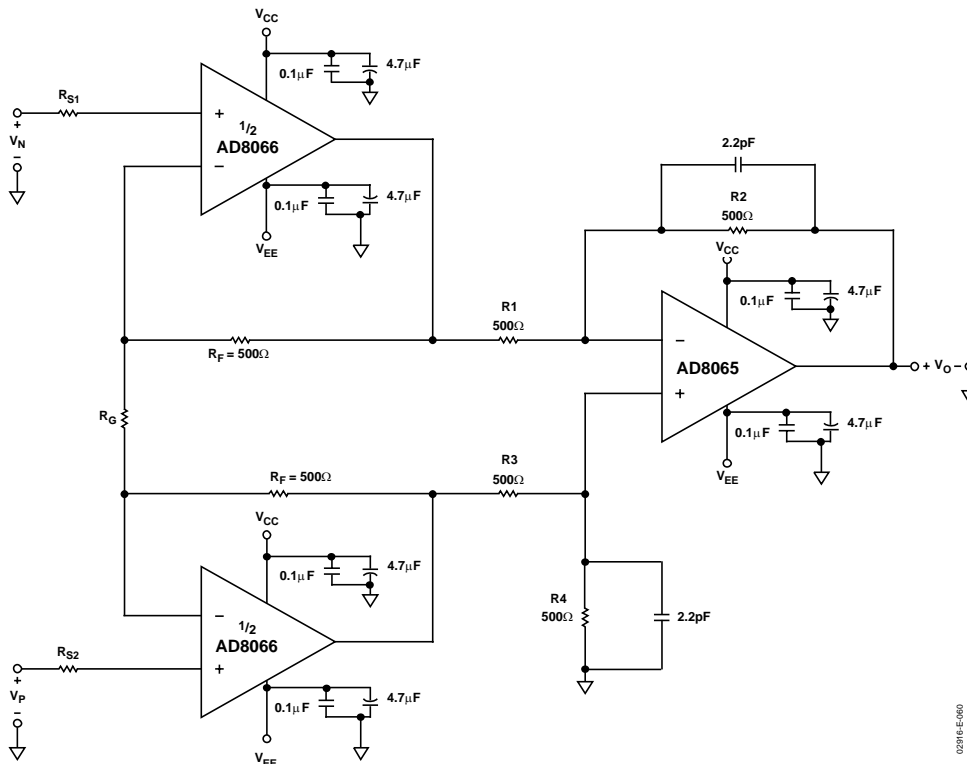


Figure 60. High Speed Instrumentation Amplifier

**HIGH SPEED JFET INPUT INSTRUMENTATION AMPLIFIER**

Figure 60 shows an example of a high speed instrumentation amplifier with high input impedance using the AD8065/AD8066. The dc transfer function is

$$V_{OUT} = (V_N - V_P) \left( 1 + \frac{1000}{R_G} \right)$$

For  $G = +1$ , it is recommended that the feedback resistors for the two preamps be set to a low value (for instance 50  $\Omega$  for 50  $\Omega$  source impedance). The bandwidth for  $G = +1$  is 50 MHz. For higher gains, the bandwidth is set by the preamp, equaling

$$Inamp_{-3dB} = (f_{CR} \times R_G) / (2 \times R_F)$$

Common-mode rejection of the in-amp is primarily determined by the match of the resistor ratios  $R1:R2$  to  $R3:R4$ . It can be estimated

$$\frac{V_O}{V_{CM}} = \frac{(\delta 1 - \delta 2)}{(1 + \delta 1) \delta 2}$$

The summing junction impedance for the preamps is equal to  $R_F \parallel 0.5(R_G)$ . This is the value to be used for matching purposes.

**VIDEO BUFFER**

The output current capability and speed of the AD8065 make it useful as a video buffer, shown in Figure 61.

The  $G = +2$  configuration compensates for the voltage division of the signal due to the signal termination. This buffer maintains 0.1 dB flatness for signals up to 7 MHz, from low amplitudes up to 2 V p-p (see Figure 7). Differential gain and phase have been measured to be 0.02% and 0.028°, respectively, at  $\pm 5$  V supplies.

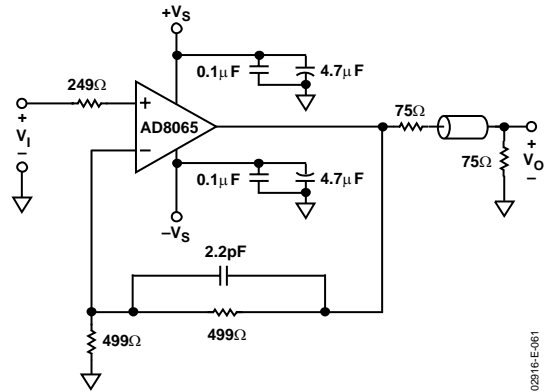
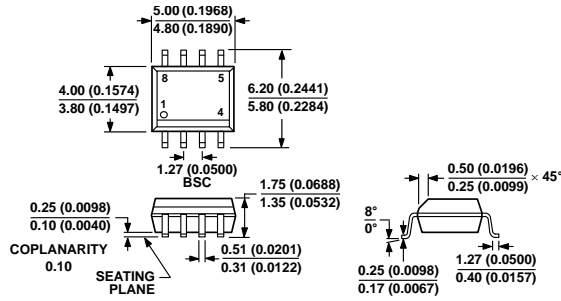


Figure 61. Video Buffer

02816E-061

OUTLINE DIMENSIONS



COMPLIANT TO JEDEC STANDARDS MS-012-AA  
 CONTROLLING DIMENSIONS ARE IN MILLIMETERS; INCH DIMENSIONS (IN PARENTHESES) ARE ROUNDED-OFF MILLIMETER EQUIVALENTS FOR REFERENCE ONLY AND ARE NOT APPROPRIATE FOR USE IN DESIGN.

Figure 62. 8-Lead Standard Small Outline Package [SOIC\_N] Narrow Body (R-8)



COMPLIANT TO JEDEC STANDARDS MO-178-AA  
 Figure 63. 5-Lead Small Outline Transistor Package [SOT-23] (RJ-5)



COMPLIANT TO JEDEC STANDARDS MO-187-AA  
 Figure 64. 8-Lead Mini Small Outline Package [MSOP] (RM-8)  
 Dimensions shown in millimeters

## ORDERING GUIDE

Model <sup>1,2</sup>	Temperature Range	Package Description	Package Option	Marking Code
AD8065ARZ	−40°C to +85°C	8-Lead SOIC_N	R-8	
AD8065ARZ-REEL	−40°C to +85°C	8-Lead SOIC_N	R-8	
AD8065ARZ-REEL7	−40°C to +85°C	8-Lead SOIC_N	R-8	
AD8065ART-R2	−40°C to +85°C	5-Lead SOT-23	RJ-5	HRA
AD8065ART-REEL7	−40°C to +85°C	5-Lead SOT-23	RJ-5	HRA
AD8065ARTZ-R2	−40°C to +85°C	5-Lead SOT-23	RJ-5	HRA#
AD8065ARTZ-REEL	−40°C to +85°C	5-Lead SOT-23	RJ-5	HRA#
AD8065ARTZ-REEL7	−40°C to +85°C	5-Lead SOT-23	RJ-5	HRA#
AD8065WARTZ-R7	−40°C to +105°C	5-Lead SOT-23	RJ-5	H2F#
AD8066ARZ	−40°C to +85°C	8-Lead SOIC_N	R-8	
AD8066ARZ-RL	−40°C to +85°C	8-Lead SOIC_N	R-8	
AD8066ARZ-R7	−40°C to +85°C	8-Lead SOIC_N	R-8	
AD8066ARMZ	−40°C to +85°C	8-Lead MSOP	RM-8	H7C
AD8066ARMZ-REEL7	−40°C to +85°C	8-Lead MSOP	RM-8	H7C

<sup>1</sup> Z = RoHS Compliant Part, # denotes RoHS compliant product may be top or bottom marked.

<sup>2</sup> W = Qualified for Automotive Applications.

## AUTOMOTIVE PRODUCTS

The AD8065W model is available with controlled manufacturing to support the quality and reliability requirements of automotive applications. Note that these automotive models may have specifications that differ from the commercial models; therefore, designers should review the Specifications  $\pm 5$  V section of this data sheet carefully. Only the automotive grade products shown are available for use in automotive applications. Contact your local Analog Devices account representative for specific product ordering information and to obtain the specific Automotive Reliability reports for these models.

Компания «Life Electronics» занимается поставками электронных компонентов импортного и отечественного производства от производителей и со складов крупных дистрибьюторов Европы, Америки и Азии.

С конца 2013 года компания активно расширяет линейку поставок компонентов по направлению коаксиальный кабель, кварцевые генераторы и конденсаторы (керамические, пленочные, электролитические), за счёт заключения дистрибьюторских договоров

Мы предлагаем:

- Конкуренспособные цены и скидки постоянным клиентам.
- Специальные условия для постоянных клиентов.
- Подбор аналогов.
- Поставку компонентов в любых объемах, удовлетворяющих вашим потребностям.
- Приемлемые сроки поставки, возможна ускоренная поставка.
- Доставку товара в любую точку России и стран СНГ.
- Комплексную поставку.
- Работу по проектам и поставку образцов.
- Формирование склада под заказчика.
- Сертификаты соответствия на поставляемую продукцию (по желанию клиента).
- Тестирование поставляемой продукции.
- Поставку компонентов, требующих военную и космическую приемку.
- Входной контроль качества.
- Наличие сертификата ISO.

В составе нашей компании организован Конструкторский отдел, призванный помогать разработчикам, и инженерам.

Конструкторский отдел помогает осуществить:

- Регистрацию проекта у производителя компонентов.
- Техническую поддержку проекта.
- Защиту от снятия компонента с производства.
- Оценку стоимости проекта по компонентам.
- Изготовление тестовой платы монтаж и пусконаладочные работы.



Тел: +7 (812) 336 43 04 (многоканальный)

Email: [org@lifeelectronics.ru](mailto:org@lifeelectronics.ru)